Ideas on $\mathrm{B}_{\mathrm{s}}^{0} \to \tau^{\pm}\tau^{\mp}$ reconstruction

LHCb Internal Note

Issue: 1
Revision: 0

Reference: LHCb-INT-2011-039
Created: May 30, 2011
Last modified: August 29, 2011

Prepared by: Fred Blanc[a], Anne Keune[a], Tatsuya Nakada[a]
[a]Laboratoire de Physique des Hautes Energies, Ecole Polytechnique Fédérale de Lausanne, Switzerland

LHCb-INT-2011-039
29/08/2011

Abstract

In this note the possibility of analytically calculating and computationally reonstructing the B_s^0 and τ momenta from the decay $\mathrm{B}_\mathrm{s}^0 \to \tau^\pm\tau^\mp$ with $\tau^\pm \to \pi^\pm\pi^\pm\pi^\mp\nu_\tau$ is discussed. After reconstruction, without any selection cuts, the calculation efficiency is determined to be approximately 33%. On average, each fully reconstructable decay gives rise to three momentum solutions. Interestingly, the lifetime distributions of the correct and incorrect momentum solutions appear equivalent.

1 Introduction

A principal goal for LHCb is the measurement of the branching fraction of the decay $\mathrm{B}_\mathrm{s}^0 \to \mu^\pm\mu^\mp$. This decay is rare in the Standard Model as it occurs only via helicity suppressed loop diagrams. Its branching fraction can be significantly different in many New Physics models, especially with an extended Higgs sector. Therefore, the search for this decay provides a sensitive probe of physics beyond the Standard Model.

The decay rates of $\mathrm{B}_\mathrm{s}^0 \to \ell^\pm\ell^\mp$ are suppressed by a factor $(m_\ell/m_B)^2$. The suppression is therefore smallest for $\mathrm{B}_\mathrm{s}^0 \to \tau^\pm\tau^\mp$, due to the large τ mass. However, reconstructing decays involving a τ lepton are experimentally challenging.

The final state of a τ lepton decay contains one or more neutrinos. In the $\mathrm{B}_\mathrm{s}^0 \to \tau^\pm\tau^\mp$ decay with both τ leptons decaying hadronically, there are two neutrino's in its final state. There is no possibility to measure the missing energy of this decay in LHCb.

However, the possible neutrino momenta, and thus τ and B_s^0 momenta, can be calculated such that all topological and kinematic constraints are satisfied. In order to perform this calculation, the decay vertices of the τ leptons need to be known. It is therefore required that both τ leptons decay into a multi-prong of charged particles, enabling the reconstruction of the decay vertices. The requirement of both τ leptons decaying as $\tau^\pm \to \pi^\pm\pi^\pm\pi^\mp\nu_\tau$ reduces the total branching fraction significantly. How to perform this calculation is the subject of this note.

The six charged hadrons in the final state causes the reconstruction efficiency to be low. In addition, it is a challenge for a decay in which the p_T is spread over six charged particles to pass any trigger. The calculation efficiency and the final selection efficiency further reduces the total efficiency, but are not uncorrelated. The efficiency of the background suppression using this calculation is yet unstudied.

Reconstructing $\mathrm{B}_\mathrm{s}^0 \to \tau^\pm\tau^\mp$ is a challenge and it is not clear that the Standard Model branching fraction can be measured within the lifetime of LHCb or its upgrade. However, the New Physics contribution may be considerable and it is well worth establishing an upper limit on the branching fraction of this decay.

2 Analytical Calculation

The measurable variables of the $\mathrm{B}_\mathrm{s}^0 \to \tau^\pm\tau^\mp$ decay with $\tau^\pm \to \pi^\pm\pi^\pm\pi^\mp\nu_\tau$ are

- the B_s^0 production vertex (primary vertex): pV,
- the two τ decay vertices: dV_1 and dV_2,

- the 4-momenta of the two three-prongs: $p_{1\mathcal{3}\pi}$ and $p_{2\mathcal{3}\pi}$.

The unknown quantities are

- the decay vertex of the B_s^0 meson: bV,
- the momentum of the B_s^0 meson: $\vec{p}_\mathrm{B}$,
- the momenta of the two τ leptons: $\vec{p}_{1\tau}$ and $\vec{p}_{2\tau}$,
- the momenta of the two neutrinos: $\vec{p}_{1\nu}$ and $\vec{p}_{2\nu}$.

The masses of the B_s^0 meson, τ leptons and neutrinos are fixed to their experimentally determined values and denoted by m_B, m_τ and m_ν. The multi-prong of the three pions is denoted by $\mathcal{3}\pi$.

When two τ leptons come from an unknown vertex, the reconstruction of their momenta is challenging. It is not possible to calculate the τ momentum without knowing the angle between the τ and $\mathcal{3}\pi$ momenta vectors [2] and it is not possible to calculate the B_s^0 decay vertex without knowing the direction of the τ momenta. A more convenient parameterization of the problem must therefore be found.

The B_s^0 decay vertex must lie within the plane spanned by the three vertices pV, dV_1 and dV_2. The vectors between the primary vertex and the first or second decay vertex are denoted by $\vec{v}$ and $\vec{w}$ respectively. The B_s^0 and τ momentum vectors are colinear with the spacial vectors between their origin and decay vertices. Scale factors, $L_{1\tau}$, $L_{2\tau}$ and L_B, are used to relate the topological direction vectors to the particle momenta. The basic geometry of the plane in which the B_s^0 and τ momenta lie is depicted in Figure 1.

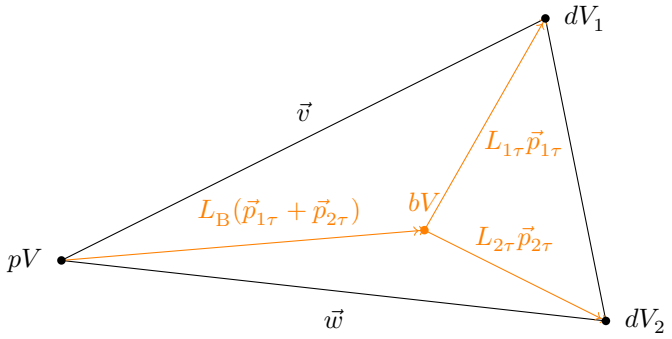

Figure 1 Geometry of the plane containing the B_s^0 and both τ momentum vectors.

The three relations linking the directional vectors to the momenta using scale factors are

$$dV_1 - bV = L_{1\tau}\vec{p}_{1\tau} \tag{1}$$
$$dV_2 - bV = L_{2\tau}\vec{p}_{2\tau} \tag{2}$$
$$bV - pV = L_\mathrm{B}(\vec{p}_{1\tau} + \vec{p}_{2\tau}) \tag{3}$$

These relations can be rewritten to a single formula, eliminating the factors $L_{1\tau}$, $L_{2\tau}$ and L_B, as

$$\vec{v} \times \vec{p}_{1\tau} = -\vec{w} \times \vec{p}_{2\tau} \tag{4}$$

The second relation occurs through the fixing of the B_s^0 mass: $(p_{1\tau} + p_{2\tau})^2 = m_\mathrm{B}^2$

$$E_{1\tau}E_{2\tau} - \vec{p}_{1\tau} \cdot \vec{p}_{2\tau} = \frac{1}{2}m_\mathrm{B}^2 - m_\tau^2 \tag{5}$$

And finally two relations due to the fixing of the neutrino mass

$$(p_{1\tau} - p_{13\pi})^2 = (p_{2\tau} - p_{23\pi})^2 = 0 \tag{6}$$

and two from fixing the τ mass

$$p_{1\tau}^2 = p_{2\tau}^2 = m_\tau^2 \tag{7}$$

The system to be solved thus consists of 8 equations and 8 unknowns, which are the two τ 4-momenta $\{p_{1\tau}, p_{2\tau}\}$. To simplify the algebra, the plane is rotated such that its norm aligns with the z-axis. By doing this the z-components of the two τ momenta as well as the vectors $\vec{v}$ and $\vec{w}$ are set to 0. From this point onwards this will be assumed to be the case.

In 2D space the system reduces to 6 equations with 6 unknowns $\{E_{1\tau}, p_{1\tau x}, p_{1\tau y}, E_{2\tau}, p_{2\tau x}, p_{2\tau y}\}$. For a better overview Equations 4-7 can be rewritten with in 2D space with substituted variables as

$$x_1^2 + y_1^2 - z_1^2 = -1 \tag{8}$$
$$a_1 x_1 + y_1 + b_1 z_1 = c_1 \tag{9}$$
$$x_2^2 + y_2^2 - z_2^2 = -1 \tag{10}$$
$$a_2 x_2 + y_2 + b_2 z_2 = c_2 \tag{11}$$
$$k x_1 + l y_1 = m x_2 + y_2 \tag{12}$$
$$x_1 x_2 + y_1 y_2 - z_1 z_2 = d \tag{13}$$

Here $x_1 = p_{1\tau x}/m_\tau$, $y_1 = p_{1\tau y}/m_\tau$ and $z_1 = E_{1\tau}/m_\tau$. Thus $a_1 = p_{13\pi x}/p_{13\pi y}$, $b_1 = -E_{13\pi}/p_{13\pi y}$ and $c_1 = (-m_\tau^2 - m_{13\pi}^2)/(2m_\tau p_{13\pi y})$. The variables x_2, y_2, z_2 and measurables a_2, b_2, c_2 are defined equivalently for the second τ lepton. From equation 5 can be derived that $d = (2m_\tau^2 - m_\mathrm{B}^2)/(2m_\tau^2)$ and from equation 4 that $k = v_y/w_x$, $l = -v_x/w_x$ and $m = -w_y/w_x$. Note that the space can still be conveniently rotated to set for instance $m = 0$ or $k = l$; here we will proceed without extra rotations applied.

Equation 8 represents a quadric: a hyperboloid of two sheets. Equation 9 is a plane. Together these two equations represent an ellipse in 3D space. This ellipse can be parameterized using one single variable, chosen to be t. To start the parameterization a point (x_0, y_0, z_0) on the ellipse is chosen. For a given value of z_0, x_0 is expressed as

$$x_0 = \frac{a_1(c_1 + b_1 z_0) \pm \sqrt{(a_1^2 + 1 - b_1^2)z_0^2 + 2b_1 c_1 z_0 - a_1^2 - b_1^2}}{1 + a_1^2} \tag{14}$$

Therefore there exists a solution for x_0 if

$$(a_1^2 + 1 - b_1^2)z_0^2 + 2b_1 c_1 z_0 - a_1^2 - b_1^2 \geq 0 \tag{15}$$

As $a_1^2 + 1 - b_1^2 < 0$ (the two components of the momentum squared are never larger than the energy squared), this represents a parabola which opens downward. It is therefore a safe choice to take

$$z_0 = \frac{-b_1 c_1}{a_1^2 + 1 - b_1^2} \tag{16}$$

as the starting value for z_0.

A pencil of planes, orthogonal to the xz-plane and crossing coordinate (x_0, y_0, z_0), can be chosen as

$$x_1 = x_0 - t\,(z_1 - z_0) \tag{17}$$

where t is the new parameter in which the ellipse is parameterized. Substituting equations 9 and 17 into equation 8 gives a quadratic solution for z_1 expressed in terms of t. One of the solutions for z_1 is known to be z_0. Cancelling out this known solution leaves a general algebraic expression for z_1 in terms of t.

$$z_1 = \frac{\left(z_0 a_1^2 + z_0\right) t^2 + 2\left(x_0 - a_1 c_1 + a_1^2 x_0\right) t + 2b_1 y_0 + b_1^2 z_0 + z_0}{\left(a_1^2 + 1\right) t^2 - 2a_1 b_1 t + b_1^2 - 1} \tag{18}$$

It follows that x_1 and y_1 can be expressed in terms of t as

$$x_1 = \frac{\left(x_0 a_1^2 - x_0 + 2a_1 y_0\right) t^2 + 2\left(b_1 c_1 + b_1^2 z_0 - z_0\right) t + b_1^2 x_0 - x_0}{\left(a_1^2 + 1\right) t^2 - 2a_1 b_1 t + b_1^2 - 1}\,, \tag{19}$$

$$y_1 = \frac{\left(-y_0 a_1^2 + y_0 + 2a_1 x_0\right) t^2 + 2\left(a_1 z_0 - b_1 x_0 + a_1 b_1 y_0\right) t - b_1^2 y_0 - y_0 - 2b_1 z_0}{\left(a_1^2 + 1\right) t^2 - 2a_1 b_1 t + b_1^2 - 1} \tag{20}$$

Both the nominator and the denominator are of order 2 in t for x_1, y_1 and z_1. In addition, the three variables share the same denominator. These expressions will be denoted by

$$x_1 = \frac{t_x}{t_n},\, y_1 = \frac{t_y}{t_n} \text{ and } z_1 = \frac{t_z}{t_n} \tag{21}$$

to retain the general overview.

Equations 11-13 are now used to express x_2, y_2 and z_2 in terms of t. The result for each variable is a fraction with both the nominator and denominator of order 4 in t.

$$x_2 = \frac{(kt_x + lt_y)(-t_z - b_2 t_y) + t_n(c_2 t_z + b_2 d t_n)}{t_n(a_2 t_z - m t_z + b_2 t_x - m b_2 t_y)} \tag{22}$$

$$y_2 = \frac{(kt_x + lt_y)(b_2 t_x + a_2 t_z) - m t_n(c_2 t_z + b_2 d t_n)}{t_n(a_2 t_z - m t_z + b_2 t_x - m b_2 t_y)} \tag{23}$$

$$z_2 = \frac{(kt_x + lt_y)(a_2 t_y - t_x) + t_n(c_2 t_x - c_2 m t_y - a_2 d t_n + m d t_n)}{t_n(a_2 t_z - m t_z + b_2 t_x - m b_2 t_y)} \tag{24}$$

Equation 10 is so far unused and substituting the expressions of x_2, y_2 and z_2 in t into this relation leaves a single polynomial of order 8 in t. This polynomial will be referred to by $p_0(t)$.

Polynomial solutions The polynomial cannot be solved analytically. However, it has the advantage that parameter t is limited to an interval of approximately $(-1, 1)$. The distribution of t is depicted in Figure 2. Algorithms exist, like the algorithm of Sturm [3], that determine the number of roots

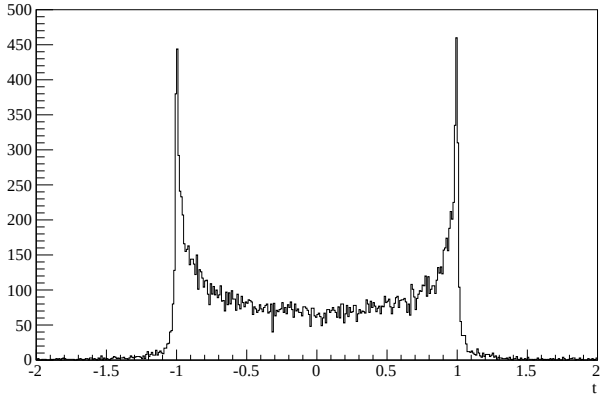

Figure 2 The distribution of parameter t as calculated from the generator-level 4-vectors of 25,000 $\mathrm{B_s^0} \to \tau^\pm\tau^\mp$ events.

within a certain interval. In order to apply Sturm's theorem the polynomial has to be expressed in its monomial basis. However, the values of the roots of $p_0(t)$ are highly sensitive to perturbations in the coefficients of the polynomial. Expressing $p_0(t)$ in its monomial basis changes the location of its roots significantly. Figure 3 shows the outcome of $p_0(t)$ before and after bracket expansion. The MC true solution of the polynomial is lost after expansion. The problem is thus ill-conditioned (similar to

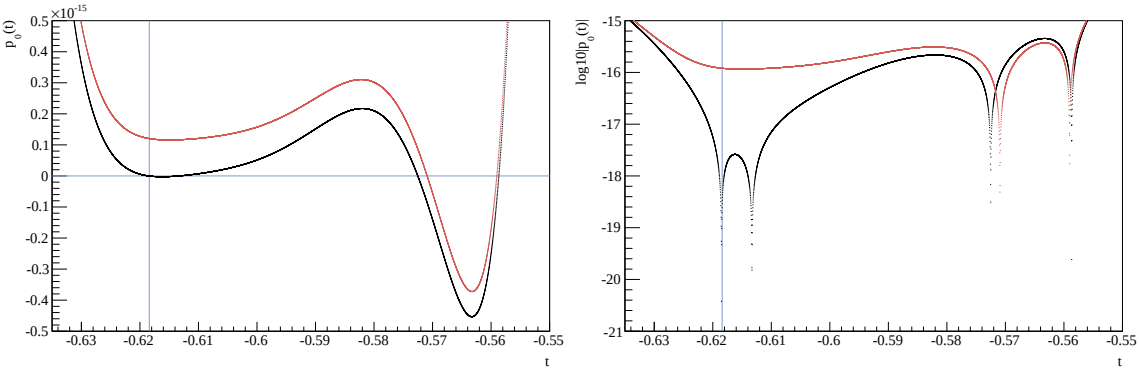

(a) (b)

Figure 3 The outcome of the polynomial p_0 as a function of t for a given event, depicted by (a) the value of $p_0(t)$ and (b) the value of $\log 10(|p_0(t)|)$. In black the original unexpanded outcome and in red the outcome after expanding to a monomial basis. The blue line represents the MC true value of parameter t.

Wilkinson's polynomial [4]). The solutions of $p_0(t) = 0$ will therefore have to be located by scanning over a specified interval in small enough steps to result into the required roots.

Although it is an 8^{th} order polynomial, it has usually 2 or 4 roots, with one of them corresponding to the MC true solution. Whether it is possible to distinguish between these solutions depends on the $\mathrm{B_s^0} \to \tau^{\pm}\tau^{\mp}$ decay specific kinematic and topological distributions. In section 2.2 the lifetime distribution is discussed.

Additional space rotations As mentioned in the previous section, an additional space rotation in the xy-plane can be made to simplify the problem. The space can be rotated such that $k = l$ or $m = 0$ for instance. This does not change the general outcome of the problem; there is still an 8^{th} order polynomial to solve. But it simplifies the formulas and effects the distribution of parameter t.

The distributions of t, for the cases $k = l$ and $m = 0$, are depicted in Figure 4. For both cases, the interval of possible t solutions has decreased compared to the case where no extra rotation is made.

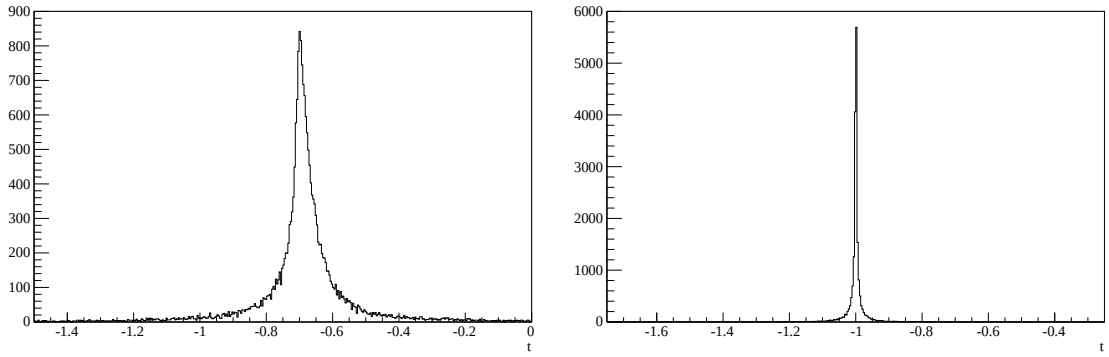

(a) (b)

Figure 4 The t distribution after the xy-plane is rotated such that (a) $k = l$ and (b) $m = 0$.

2.1 Accuracy and Efficiency

The accuracy and efficiency of the solutions found by solving $p_0(t) = 0$ are dependent of the step size, δt , which is used to scan over the pre-defined interval $[t_{\text{min}}, t_{\text{max}}] = [-2, 2]$ of possible solutions. For different step sizes, the calculation efficiency, ϵ_{cal}, and the average number of roots found are given in Table 1. The efficiency is given by the percentage of decays for which at least one solution can be found for $p_0(t) = 0$, i.e. more than one solution per decay does not increase the efficiency. As shown in Table 1, the efficiency increases as the step size decreases. At the same time, the average number of roots increases. Additional real roots are found, but also duplicate roots are calculated as the value of $p_0(t)$ may fluctuate around zero due to rounding errors, when there is only one true root.

δt	ϵ_{cal}	roots
0.01	72.7%	2.529
0.005	80.5%	2.638
0.002	87.6%	2.749
0.001	90.7%	2.806
0.0005	92.4%	2.847
0.0002	93.5%	2.893
0.0001	93.9%	2.943
0.00005	94.1%	3.042
0.00002	94.1%	3.350

Table 1 The calculation efficiency, ϵ_{cal}, and the average number of roots found for different values of δt.

Figure 5 depicts the resolution between the MC value of t and the calculated value of t which is closest to the MC truth (referred to as the best calculated value). To better depict the differences, the logarithm of the absolute value of the resolution is taken. For larger step sizes, the resolution is dominated by the step size. This results in the peak structures in Figure 5. For $\delta t = 0.00002$, this peak structure is negligible and for $\delta t = 0.00005$ it has completely saturated.

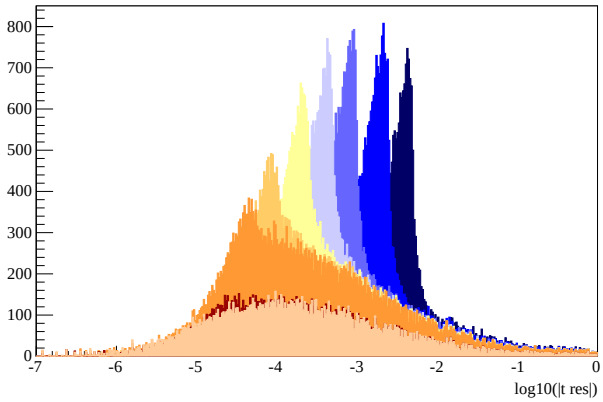

Figure 5 The difference between the MC value of t and the best calculated value of t for step sizes $\delta t = 0.01$ to $\delta t = 0.00002$ (as in Table 1) ranging in colour from dark blue to light orange.

However, it is also important to keep in mind the speed of the program. As the efficiency does not increase much for step sizes smaller than 0.0001 and as the effect on the resolution is limited, it is chosen to continue this study with δt = 0.0001. The plots shown and results quoted hereafter are thus based on the solutions found when using δt = 0.0001.

Although the parameter interval $[t_{\text{min}}, t_{\text{max}}]$ after an extra space rotation is significantly reduced, it is not necessarily advantageous to do so. As the same number of solutions occur on a smaller interval, there are more fluctuations around zero. In the case of the extra space rotation such that $m = 0$, the average number of roots found for δt = 0.0002 is 1.7, whereas for δt = 0.00002 it is 14.3. Although it is

a route which can be explored further, no extra space rotations are made to obtain the results in this note.

2.1.1 Generation Level

By solving $p_0(t) = 0$ possible τ lepton momenta, $\mathrm{B_s^0}$ momentum and $\mathrm{B_s^0}$ decay vertices are determined that satisfy all topological and kinematic constraints. However, only one of the solutions corresponds best to the MC truth. The solution which corresponds best to the MC truth based on the t resolution (referred to as the best solution) is chosen to determine the accuracy with which the variables $|\vec{p}_\tau|$, $|\vec{p}_\mathrm{B}|$ and bV can be calculated. Here, the MC generated values of the momenta and vertices are used to calculate the solutions.

Figure 6 shows the asymmetries $A(|\vec{p}_\tau|)$ and $A(|\vec{p}_\mathrm{B}|)$ of the τ and $\mathrm{B_s^0}$ momenta, where

$$A(|\vec{p}|) = \frac{|\vec{p}| - |\vec{p}_\mathrm{MC}|}{|\vec{p}| + |\vec{p}_\mathrm{MC}|} \tag{25}$$

An asymmetry of $2.0 \cdot 10^{-4}$ for the τ momentum and $2.9 \cdot 10^{-4}$ for the $\mathrm{B_s^0}$ momentum corresponds to an error of 0.04% and 0.06% respectively.

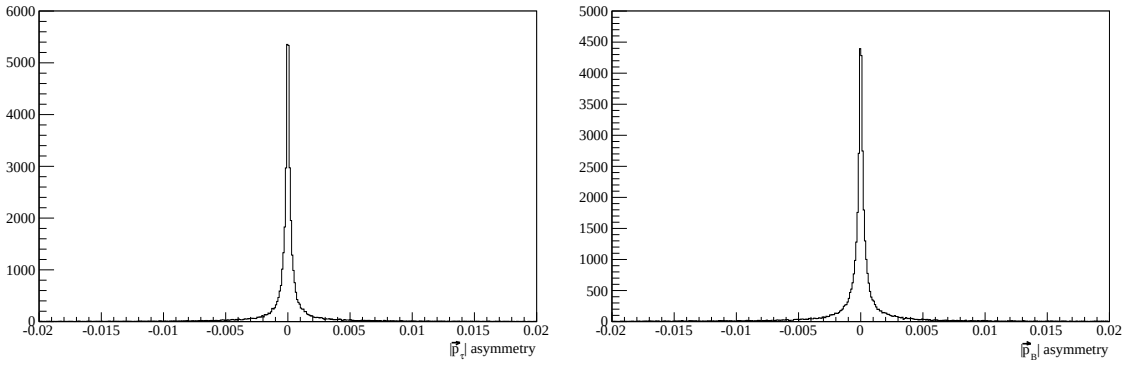

(a) FWHM = $2.0 \cdot 10^{-4}$ (b) FWHM = $2.9 \cdot 10^{-4}$

Figure 6 The (a) $|\vec{p}_\tau|$ and (b) $|\vec{p}_\mathrm{B}|$ asymmetries between the best calculated momentum and the MC true momentum.

In Figure 7 the resolutions of the $\mathrm{B_s^0}$ decay vertex are depicted. Note that only the x-component, bV_x, and y component, bV_y, are depicted, as space has been rotated such that the z-component of the $\mathrm{B_s^0}$ decay vertex is equal to the z-component of the primary vertex and is therefore fixed. These x and y-components are thus not the conventional x and y-components of the LHCb frame. Resolutions of 0.30 μm in x and 0.42 μm in y are obtained.

2.1.2 Reconstruction Level

In this section, reconstructed particles that match MC particles from the signal decay are selected. Before the efficiency of the calculation can be determined, the reconstruction efficiency needs to be considered. The reconstruction efficiency is the percentage of decays for which all six final state pions are reconstructed in LHCb. The MC data sample solely contains events for which all decay daughters travel within 400 mrad of the beam axis. Of these events approximately 5.7% is fully reconstructed in LHCb. No cuts on the reconstructed particles have been made.

When fully reconstructed, 47% of decays can be formulated by the polynomial $p_0(t)$. The likelihood of finding a solution is approximately 33%. That means, in 33% of the events, one or more roots of

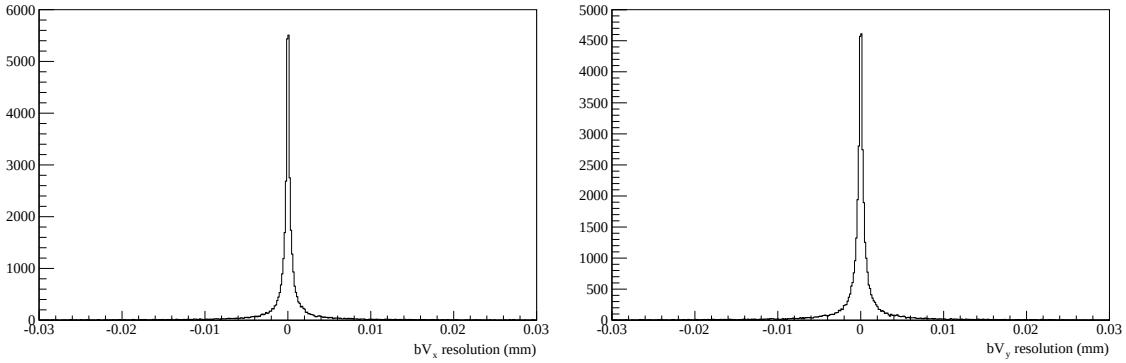

(a) FWHM = $3.0 \cdot 10^{-4}$ mm (b) FWHM = $4.2 \cdot 10^{-4}$ mm

Figure 7 The (a) bV_x and (b) bV_y resolution between the best calculated vertex and the MC true vertex.

the polynomial $p_0(t)$ can be determined. The remaining 14% of decays results in a valid polynomial, but no roots are found. For the other 53% of the cases, either the system of Equations 8 and 9 or of Equations 10 and 11 does not have an analytical solution. The plane of possible τ momenta that obey the τ mass constraint does not intersect the hyperboloid of possible momenta that obey the neutrino mass constraint. Therefore an ellipse cannot be constructed nor parameterized.

Figure 8 shows the asymmetries $A(|\vec{p}_\tau|)$ and $A(|\vec{p}_\mathrm{B}|)$ of the reconstructed τ and $\mathrm{B_s^0}$ momenta. The FWHM of the distributions are 0.07 and 0.06, which corresponds to an error of 15% and 13% respectively.

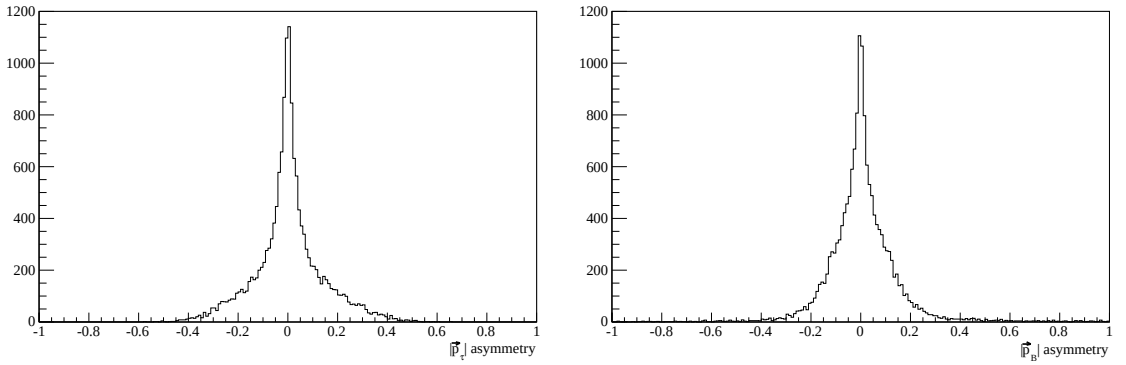

(a) FWHM = 0.07 (b) FWHM = 0.06

Figure 8 The (a) $|\vec{p}_\tau|$ and (b) $|\vec{p}_\mathrm{B}|$ asymmetries between the best reconstructed momentum and the MC true momentum.

In Figure 9 the resolutions of the $\mathrm{B_s^0}$ decay vertex are depicted. Resolutions of 1.4 mm in x and 1.8 mm in y are obtained.

The calculation efficiency and selection efficiency are not uncorrelated. It is likely that in any selection only decay vertices are selected which are sufficiently distant from the primary vertex. Figure 10 shows the different vertex distance distributions of the decays with and without a successfully calculated solution. It is shows that for small distances between the primary vertex and either of the τ decay vertices, it is less likely to find a solution. When a cut is made at $|dV_z - pV_z| > 4$ mm for both vertices, the calculation efficiency for the remaining candidates goes up from 33% to 42%. The momenta assymetries are not notably effected by this cut. Additional selection cuts may improve the calculation efficiency further.

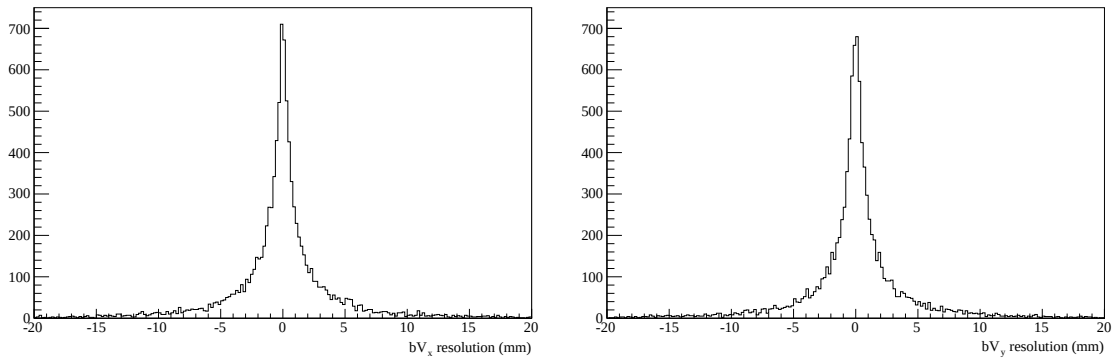

(a) FWHM = 1.4 mm (b) FWHM = 1.8 mm

Figure 9 The (a) bV_x and (b) bV_y resolution between the best reconstructed vertex and the MC true vertex.

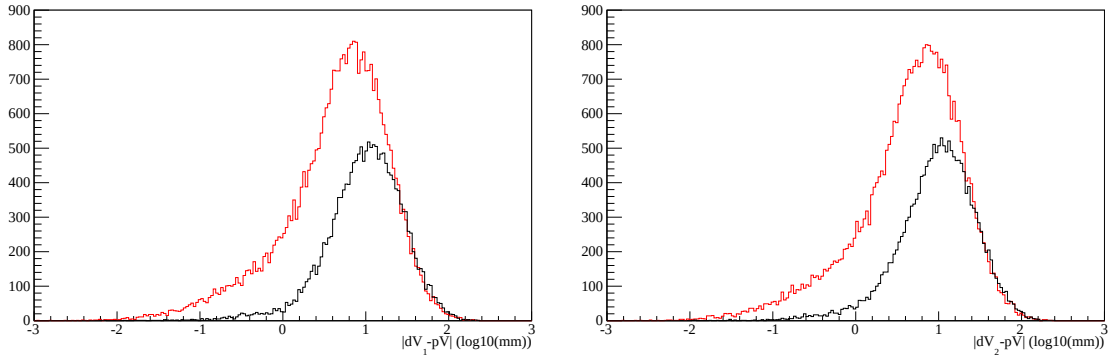

(a) (b)

Figure 10 The distances between the primary vertex and the (a) τ_1 decay vertex and the (b) τ_2 decay vertex. In black the distances of the decays for which a solution was successfully calculated and in red the distances of the decays for which no solution was found.

2.2 Lifetime distributions

Generally there are 2 or 4 possible $\mathrm{B_s^0}$ vertices, of which only one matches the MC true vertex. Whether it is possible to distinguish between correct and incorrect solutions will be dependent on the decay specific distributions of kinematic and topological variables. In this section, only the lifetime distributions of the τ lepton and $\mathrm{B_s^0}$ meson are discussed. The τ lifetime value is $\tau_\tau = (2.906 \pm 0.010) \cdot 10^{-13}$ s, whereas the $\mathrm{B_s^0}$ lifetime is $\tau_\mathrm{B} = (1.452 \pm 0.041) \cdot 10^{-12}$ s, as stated by the PDG [5].

In Figures 11 and 12 the τ and $\mathrm{B_s^0}$ distributions of the calculated lifetime on generation level are depicted. The figures show the τ and $\mathrm{B_s^0}$ lifetime distributions of (left) the best calculated solutions and of (right) the of the remaining solutions. The best calculated solutions correspond to those of which parameter t differs least from its MC value. Figure 13 shows (left) the τ and (right) the $\mathrm{B_s^0}$ lifetime distribution of the reconstructed particles for the best calculated solutions in black and for the remaining solutions in blue (scaled). Although there are differences between the distributions, they are not large enough to distinguish between solutions and are negligible for reconstructed data.

It can be concluded that the lifetime distributions of the best and remaining reconstructed particles are indistinguishable. To model the lifetime distribution, it is therefore unnecessary to determine the correct solution. The different lifetimes found per event can be weighted according to the number of solutions found. The result will be the same lifetime distribution.

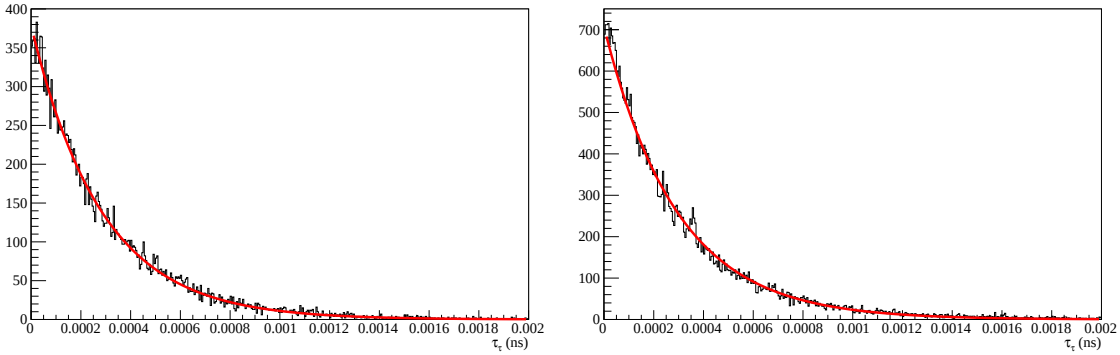

(a) $\tau_\tau = (2.826 \pm 0.020) \cdot 10^{-13}$ s. (b) $\tau_\tau = (2.934 \pm 0.016) \cdot 10^{-13}$ s.

Figure 11 The lifetime distribution of (a) the set of best τ momentum solutions and (b) the set of remaining τ momentum solutions calculated on generation level. In red the exponential functions fitted to the data.

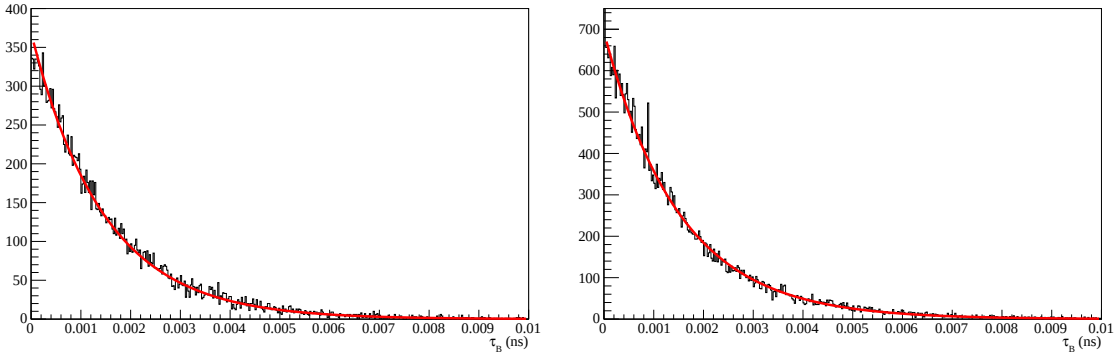

(a) $\tau_{\mathrm{B}} = (1.451 \pm 0.010) \cdot 10^{-12}$ s. (b) $\tau_{\mathrm{B}} = (1.510 \pm 0.008) \cdot 10^{-12}$ s.

Figure 12 The lifetime distribution of (a) the set of best $\mathrm{B}_{\mathrm{s}}^0$ momentum solutions and (b) the set of remaining $\mathrm{B}_{\mathrm{s}}^0$ momentum solutions calculated on generation level. In red the exponential functions fitted to the data.

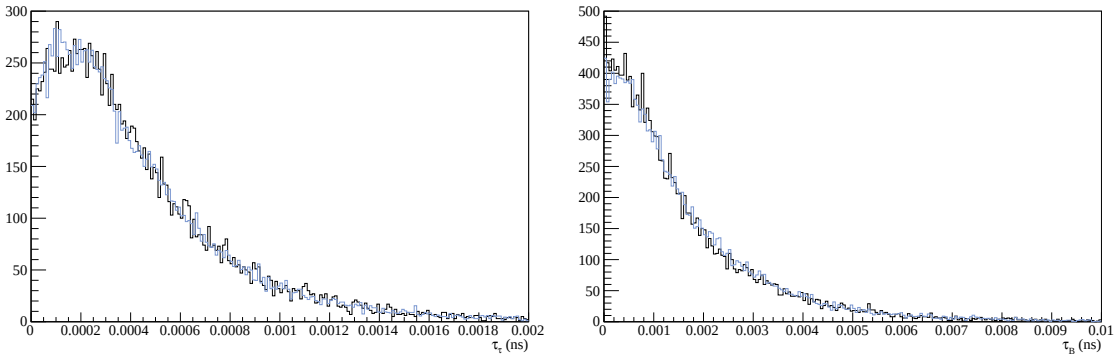

(a) (b)

Figure 13 The lifetime distributions of (a) the τ momentum solutions and (b) the $\mathrm{B}_{\mathrm{s}}^0$ momentum solutions calculated on reconstruction level. The lifetime distribution of the set of best calculated momenta is drawn in black and the lifetime distribution of the set of remaining momenta in blue (scaled).

3 Computational Reconstruction

A constraint fit exploits the errors on the measured quantities to find the best fitting τ momenta when an exact calculation is not possible. Its aim is to minimise the value of the χ^2, defined as

$$\chi^2 = (m - h(x))^T W (m - h(x)) \tag{26}$$

The measured values are denoted by m. The model, $h(x)$, contains the calculated values of the measured quantities based on parameters x. W is the weight matrix; the inverse of the covariance matrix of the measured quantities.

The model and its parameters need to be chosen carefully to ensure convergence to a minimum χ^2 value. The standard measured quantities are the primary vertex, pV, and for both τ leptons the decay vertex, dV, and the 3π 4-momentum, $(E_{3\pi}, \vec{p}_{3\pi})$. In addition, the combined momentum of the 6 pions, $(E_{6\pi}, \vec{p}_{6\pi})$, and its (imaginary) vertex, dV_3, is calculated. Although these values do not correspond to the vertex and momentum of a real particle, they help to constrain the problem. A small variation of the 3π energy and its momentum can lead to a negative 3π mass. It is therefore more stable to use the 3π mass in the model rather than its energy and a convenient choice of variable is $m^2_{3\pi}$. The same holds for the 6π mass. The chosen model consists of the following 24 quantities

$$h(x) = \left\{ pV, dV_1, \vec{p}_{1\,3\pi}, m^2_{1\,3\pi}, dV_2, \vec{p}_{2\,3\pi}, m^2_{2\,3\pi}, dV_3, \vec{p}_{6\pi}, m^2_{6\pi} \right\} \tag{27}$$

The Jacobian matrix is applied to the covariance matrix in order to make it compatible with the change of variable. The vertices and momenta of the measured variables together with their components in the covariance matrix are rotated such that the z-components of the B^0_s and τ momenta are 0.

The floating parameters which are chosen to describe the model are the primary vertex, pV, the three scale factors, $L_{1\tau}$, $L_{2\tau}$ and L_B, the τ momenta, $\vec{p}_{1\tau}$ and $\vec{p}_{2\tau}$, the neutrino momenta $\vec{p}_{1\nu}$ and $\vec{p}_{2\nu}$ and the 6π vertex, dV_3. There are thus 19 parameters.

$$x = \left\{ pV, L_{1\tau}, L_{2\tau}, L_\mathrm{B}, p_{1\tau x,y}, \vec{p}_{1\nu}, p_{2\tau x,y}, \vec{p}_{2\nu}, dV_3 \right\} \tag{28}$$

The τ masses are fixed by defining $E_\tau = \sqrt{m_\tau^2 + |\vec{p}_\tau|^2}$. The relation used to describe the 3π mass

$$m^2_{3\pi} = m^2_\tau - 2E_\tau|\vec{p}_\nu| + 2\vec{p}_\tau \cdot \vec{p}_\nu \tag{29}$$

fixes the neutrino masses to 0. The 6π mass is used to then fix the B^0_s mass.

$$\begin{aligned} m^2_{6\pi} = m^2_B &- 2|\vec{p}_{1\nu}|\sqrt{m^2_\mathrm{B} + |\vec{p}_{1\tau} + \vec{p}_{2\tau}|^2} + 2\vec{p}_{1\nu} \cdot (\vec{p}_{1\tau} + \vec{p}_{2\tau}) \\ &- 2|\vec{p}_{2\nu}|\sqrt{m^2_\mathrm{B} + |\vec{p}_{1\tau} + \vec{p}_{2\tau}|^2} + 2\vec{p}_{2\nu} \cdot (\vec{p}_{1\tau} + \vec{p}_{2\tau}) \\ &+ 2|\vec{p}_{1\nu}||\vec{p}_{2\nu}| - 2\vec{p}_{1\nu} \cdot \vec{p}_{2\nu} \end{aligned} \tag{30}$$

The topological constraints are satisfied by

$$dV_1 = pV + L_\mathrm{B}(\vec{p}_{1\tau} + \vec{p}_{2\tau}) + L_{1\tau}\vec{p}_{1\tau} \tag{31}$$

$$dV_2 = pV + L_\mathrm{B}(\vec{p}_{1\tau} + \vec{p}_{2\tau}) + L_{2\tau}\vec{p}_{2\tau} \tag{32}$$

Two methods of minimisation are considered. The first uses TMinuit [6], a pre-programmed minimisation algorithm. The second is the Newton-Raphson method, which tries to find the root of the χ^2 derivative. Both methods rely on a well chosen initial guess of the parameter values to avoid getting stuck in local minima.

As discussed in section 2.1.2, approximately 47% of the decay can be described by a polynomial $p_0(t)$. For these cases, a good initial guess can be set where this polynomial is or is close to 0. For all other cases, it is much harder to set an initial guess close to a valid solution.

3.1 Fit Result and Efficiency

The fit methods are used consecutively; i.e. if the problem does not converge with one of the methods, the other method is applied. These results are thus based on the best combined result of the two fit methods. TMinuit has the advantage that lower and upper limits can be set for each variable. This makes it transparent when a parameter tends to a boundary.

For 24 degrees of freedom, the χ^2 distribution theoretically obeys the following proportions

	90%	95%	99%
χ^2	33.2	36.4	42.0

In this study, for a $\chi^2 < 33.2$, the fit efficiency is 43%. The χ^2 of many decays does therefore not reduce to its global minimum, which must be due to an insufficient initial guess. The solutions of the decays which have converged to a small χ^2 must be verified to be valid solutions.

Figure 14 depicts the MC distributions of scale factors L_B and L_1 (which is equivalent to the distribution of L_2). Based on this distribution, the lower and upper limits of the TMinuit constraints for all scale factors have been set to 10^{-7} and 10^{-3} respectively. The solution is expected within these limits.

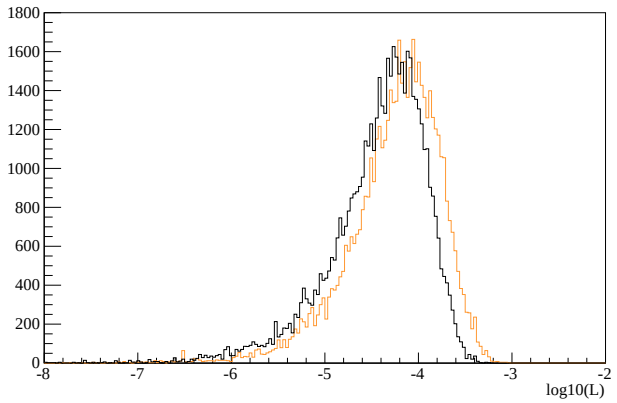

Figure 14 The MC values of the scale factors L_B (orange) and $L_{1\tau}$ (black).

Figure 15 shows that the L_B scale factor often tends to zero during the fitting process. The same is true for the $L_{1\tau}$ and $L_{2\tau}$ scale factors. The χ^2 value in this case can be sufficiently low, but represents a faulty solution. As can be seen in Figure 15(b), the lifetime then also approaches zero. These solutions should therefore not be taken into account when calculating the fit efficiency. When a scale factor tends to zero, the topological constraint on either the B_s^0 or on one of the τ momenta disappears and the particles 'decouple', which results in an invalid solution with a low χ^2.

Eliminating the fit solutions where one of the scale factors has gone below 10^{-6} leaves a fit efficiency of 33%. This is equivalent to the calculation efficiency.

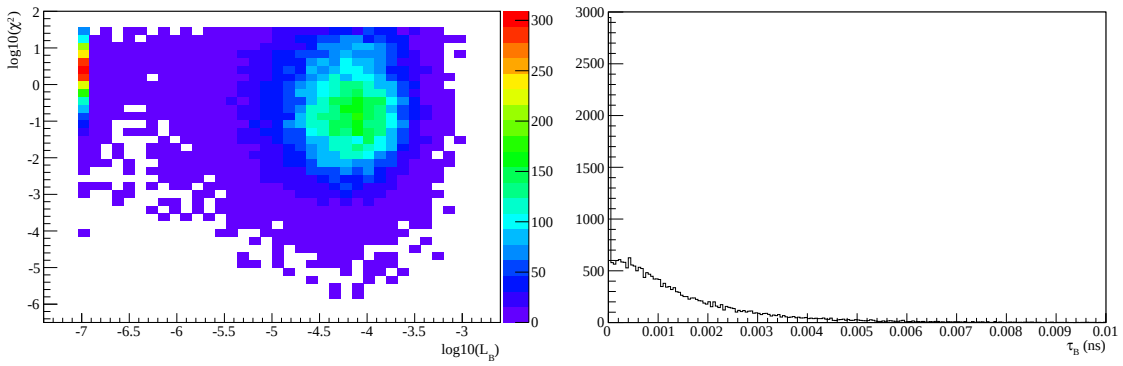

(a) (b)

Figure 15 (a) The value of $\log 10(\chi^2)$ versus the scale factor value $\log 10(L_{\rm B})$. (b) The lifetime distribution of the $\rm B_s^0$ momenta obtained by refitting the signal decay.

4 Conclusions

The $\rm B_s^0 \to \tau^\pm\tau^\mp$ decay with $\tau^\pm \to \pi^\pm\pi^\pm\pi^\mp\nu_\tau$ is theoretically reconstructable up to an $8^{\rm th}$ order polynomial. In order to find the $\rm B_s^0$ and τ momenta solutions, the roots of this polynomial need to be determined. These roots are limited to a specified interval and can be calculated by scanning this interval in a certain number of steps.

The efficiency of this calculation is approximately 33%. However, no selection cuts are made prior to the calculation. It has been shown that the calculation efficiency and the selection efficiency are not uncorrelated. Therefore the final calculation efficiency cannot be determined until a selection has been established.

Albeit an $8^{\rm th}$ order polynomial, it generally inhibits either 2 or 4 roots. Only one of these roots matches with the MC truth. Whether it is possible to distiguish between the solutions is dependent on the decay specific topological and kinematic characteristics. The lifetime distributions for all found solutions are equivalent and do not give any information on which solution best matches the MC truth. As the distributions are equivalent, it is not necessary to chose one of the solutions. The lifetime solutions can be weighted according to the number of roots found for the decay.

Exploiting the errors on the measured quantities by using a fit method has not been beneficial to the overall efficiency. Perhaps it is possible to avoid the tendency of the scale factors to reduce to zero by formulating the model differently. There may also be a better educated initial guess that can be used by the fit programs, which does not use the calculation described in Section 2.

Reconstructing $\rm B_s^0 \to \tau^\pm\tau^\mp$ remains a challenge, but is not impossible. Further study needs to be performed in order to fully understand the possibilities and restrictions of the signal reconstruction, in addition to its efficiency on background reduction.

The Standard Model predicts a branching fraction of $\mathcal{B}(\rm B_s^0 \to \tau^\pm\tau^\mp) = 8.9 \times 10^{-7}$ [7]. This is a factor of approximately $(m_\tau/m_\mu)^2$ larger than the $\rm B_s^0 \to \mu^\pm\mu^\mp$ branching fraction, due to helicity suppression. Taking into account that both tau leptons have to decay into three pions and a neutrino reduces the benefit to a factor 2.3. At LHCb the trigger efficiency can be estimated to be $\sim$20% and the reconstruction efficiency is approximately 5.7%. This reduces the number of relevant $\rm B_s^0 \to \tau^\pm\tau^\mp$ events reconstructed in LHCb to be 2.6% of the $\rm B_s^0 \to \mu^\pm\mu^\mp$ events, before the selection process starts.

5 References

[1] The LHCb Collaboration, R. Aaij et al, "Search for the rare decays $\mathrm{B_s^0} \to \mu^\pm\mu^\mp$ and $\mathrm{B^0} \to \mu^\pm\mu^\mp$", arXiv:1103.2465, 2011

[2] Anne Keune, "A first consideration of the decay channel $\tau^\pm \to \pi^\pm\pi^\pm\pi^\mp\nu_\tau$ as prompt τ normalisation channel", LHCb-INT-2009-030

[3] C. Sturm, "Mémoire sur la résolution des équations numériques", Bull. des sciences de Férussac 11, 1929

[4] J. H. Wilkinson, "Rounding Errors in Algebraic Processes", Englewood Cliffs, New Jersey: Prentice Hall., 1963

[5] K. Nakamura et al. (Particle Data Group), J. Phys. G 37, 075021, 2010

[6] http://root.cern.ch/root/html/TMinuit.html

[7] Y. Grossman, Z. Ligeti and E. Nardi, Phys. Rev. D 55 (1997) 2768